



Aigner, AA., Champneys, AR., & Rothos, VM. (2003). *A new barrier to the existence of moving kinks in Frenkel Kontorova lattices*.  
[https://doi.org/10.1016/S0167-2789\(03\)00261-6](https://doi.org/10.1016/S0167-2789(03)00261-6)

Early version, also known as pre-print

Link to published version (if available):  
[10.1016/S0167-2789\(03\)00261-6](https://doi.org/10.1016/S0167-2789(03)00261-6)

[Link to publication record in Explore Bristol Research](#)  
PDF-document

## University of Bristol - Explore Bristol Research

### General rights

This document is made available in accordance with publisher policies. Please cite only the published version using the reference above. Full terms of use are available:  
<http://www.bristol.ac.uk/red/research-policy/pure/user-guides/ebr-terms/>

# A new barrier to the existence of moving kinks in Frenkel Kontorova lattices

A. A. Aigner<sup>a,b</sup>, A. R. Champneys<sup>b,\*</sup> and V. M. Rothos<sup>a</sup>

<sup>a</sup>*Department of Mathematical Sciences, Loughborough University, Loughborough LE11 3TU, UK.*

<sup>b</sup>*Department of Engineering Mathematics, University of Bristol, Bristol, BS8 1TR, UK.*

---

## Abstract

An explanation is offered for an observed lower bound on the wave speed of travelling kinks in Frenkel Kontorova lattices. Kinks exist at discrete wavespeeds within a parameter regime where there is a resonance with linear waves (phonons). However, they fail to exist even in this codimension-one sense whenever there is more than one phonon branch in the dispersion relation; inside such bands only quasi-kinks with non-decaying oscillatory tails are possible. The results are presented for a discrete sine-Gordon lattice with an onsite potential that has a tunable amount of anharmonicity. Novel numerical methods are used to trace kinks with topological charge  $Q = 1$  and 2 in three parameters representing the propagation speed, lattice discreteness and anharmonicity. Although none of the analysis is presented as rigorous mathematics, numerical results suggest that the bound on allowable wavespeeds is sharp. The results also explain why the vanishing, at discrete values of anharmonicity, of the Peierls-Nabarro barrier between stationary kinks as discovered by Savin *et al*, does not lead to bifurcation of kinks with small wave speed.

*Key words:* kinks, topological solitons, discrete sine-Gordon equation, nonlinear lattices, dispersion relations, anharmonicity, numerical continuation.

---

## 1 Introduction

Frenkel Kontorova (FK) lattices have been studied as models for atomic chains, dislocations, charge density waves, magnetic and ferromagnetic domain walls

---

\* Corresponding author.

*Email address:* A.R.Champneys@bristol.ac.uk (A. R. Champneys).

in condensed matter physics and for parallel coupled one-dimensional Josephson junction arrays (see [16,26,5,31] and references therein). They also arise as discrete versions of nonlinear Klein-Gordon equations with periodic on-site potentials, where the second-difference operator is replaced by a second derivative. There are also higher-order lattice models, where the linear second difference operator is replaced by a (sometimes nonlinear) inter-site potential that may include longer-range interactions than pure nearest neighbour, which is a more realistic models for atomic chains [25]. The potentials involved are chosen such that the continuum model supports both stationary and moving defects (kinks or anti-kinks) with topological charge  $Q = 1$ . That is, the kinks connect 0 to  $2\pi$  (or vice versa) in the usual dimensionless form of potential adopted in the literature – the so-called sine-Gordon lattice.

Intuitively, it is clear that there can be stationary  $Q = 1$  kinks in the discrete lattice versions of such models which can have their midpoint centred on either a lattice point (‘site centred’) or midway between two sites (‘bond centred’), see Sec. 2.3 below. The discreteness leads to the so-called Peierls-Nabarro energy barrier between the site-centred and bond-centred kinks, which precludes the existence of moving kinks unless they have sufficient energy to overcome this barrier [26,11]. Otherwise moving kinks generate radiation and eventually stop, although permanent-form moving kinks can exist provided they reside on an oscillating background [13]. Such oscillating-tail solutions have variously been called nanopterons, weakly nonlocal or generalised solitary waves, or quasi-solitons in the literature [3,34]. Here we shall refer to them as *quasi-kinks*.

Nevertheless, stable moving topological defects without an oscillating background, have been observed in FK lattices both experimentally and numerically. Specifically, Peyrard and Kruskal [26] found that defects with  $Q = 2$  ( $4\pi$ -kinks) can propagate stably through the sine-Gordon lattice for a range of wave speeds. Various theories have been put forward for the existence of such kinks, which rely on the fact that they are formed as bound-states of two  $2\pi$ -kinks – each cancelling out the Peierls-Nabarro barrier of the other. Also, Savin *et al.* [29] showed that with the introduction of anharmonicity in the on-site potential, the Peierls-Nabarro barrier may completely vanish, leading to the possibility of moving  $2\pi$ -kinks (a result we shall revisit in Sec. 2.3 below). Also, various special discretisations of the sine-Gordon equations exist that lead to completely integrable lattice equations, for which the barrier vanishes exactly and moving kinks exist freely for a range of wave speeds [30]. In this paper we shall deal exclusively with generic, non-integrable lattice equations. Other theories rely on the addition of forcing and damping – e.g. This can result in ‘bunched fluxons’ where the travelling kinks have leading damped oscillatory tails, as has been observed in Josephson junction arrays [32] and in simulations of models of interacting atoms [6]. In this paper, we shall consider the pure form of the FK lattice, without damping or external forcing.

The specific model we take is as follows. Consider a chain of coupled particles a fixed distance  $d$  apart with external on-site potential. The dimensionless Hamiltonian is assumed to be of the form

$$H = \sum_{n \in \mathbb{Z}} \left[ \frac{1}{2} p_n^2 + U(u_{n+1} - u_n) + \gamma W(u_n; \alpha) \right], \quad (1)$$

where  $u_n$  is the displacement of the  $n$ th particle from its equilibrium position,  $u_{n+1} = u_n(x + d)$  and  $p_n = \dot{u}_n$  is the conjugate momentum of the  $n$ th particle in the chain. The inter-particle interaction potential  $U(r)$  is normalised by  $U(0) = 0$  and  $U''(0) = 1$ . Here we shall take a simple quadratic interaction potential, but assume the on-site potential  $W$  to be the sine potential with a tunable amount of anharmonicity, as considered in [29,27]. That is

$$U(r) = \frac{r^2}{2}, \quad W(u; \alpha) = \frac{(1 + 2\alpha)(1 - \cos u)}{1 + \alpha(1 - \cos u)}, \quad (2)$$

where  $\alpha = 0$  corresponds to the harmonic on-site potential. The parameter  $\gamma$  represents the ratio between the onsite and inter-site potentials, and, without loss of generality, space and time scales are chosen so that  $d = 1$  and the coefficient of  $\ddot{u}$  is unity.

From the Hamiltonian then follows the discrete lattice equation

$$\ddot{u}_n = u_{n+1} - 2u_n + u_{n-1} - \gamma W'(u_n; \alpha), \quad n \in \mathbb{Z}, \quad (3)$$

where  $\gamma$  measures the onsite potential strength and  $\alpha$  measures the degree of anharmonicity. Note that

$$W'(u; \alpha) = \frac{(1 + 2\alpha) \sin u}{[1 + \alpha(1 - \cos u)]^2}.$$

Taking  $\alpha = 0$  this results in the nonlinear lattice potential  $W'(u; \alpha) = \sin u$  which gives the discrete sine-Gordon equation [26], related (in the limit  $d \rightarrow 0$ ) to the usual continuum sine-Gordon equation

$$u_{tt} = u_{xx} - \sin(u). \quad (4)$$

In the limit  $\alpha \rightarrow \infty$  we get the spiked force term

$$W'(u; \infty) = 2 \sum_{m \in \mathbb{Z}} \delta(2m\pi).$$

Looking for travelling-wave solutions of permanent profile in a moving reference frame with speed  $s$  one can write

$$u_n(t) = u(n - st) = u(z), \quad z = n - st.$$



Then the Klein-Gordon equation reduces to

$$s^2 u''(z) = u(z+1) - 2u(z) + u(z-1) - \gamma W'(u(z); \alpha), \quad (5)$$

where  $'$  represents differentiation with respect to  $z$ . Note that (3) is an advance-delay differential equation that does not make sense as an initial value problem. We shall be interested in localised solutions (representing defects in the lattice). That is, solutions with boundary conditions

$$u(z) \rightarrow 2m_1\pi, \quad \text{as } z \rightarrow -\infty, \quad u(z) \rightarrow 2m_2\pi, \quad \text{as } z \rightarrow +\infty, \quad (6)$$

where  $m_1$  and  $m_2$  are arbitrary integers. If  $m_1 \neq m_2$  then the defects have a non-zero ‘topological charge’  $Q = |m_1 - m_2|$ . Such solutions are referred to as *kinks* if  $m_1 < m_2$  and *anti-kinks* if  $m_1 > m_2$ . From the mathematical point of view the distinction is somewhat arbitrary because (5) is reversible, that is invariant under  $z \rightarrow -z$ . Hence whenever a kink solution exists, so does its mirror image anti-kink.

The point of this paper is to investigate the claims in the literature about existence (and stability) of moving kink solutions to (3). The outline is as follows. In Sec. 2 we revisit a simplified theory due to [8], that suggests a form of necessary condition for the formulation of kink solutions to (5). This theory is seen in the light of that of embedded solitons, which relates properties of the dispersion relation of the lattice equation to the spectrum of the linearised advance-delay operator. This shows the existence of ‘multi-phonon bands’, which are forbidden parameter regions for the generic existence of kinks, and which accumulate on  $s = 0$ . Section 3 then goes on to study the existence of kink solutions by numerical continuation applied to the advance-delay equation (5), using an adaptation of the numerical method presented in [29]. We find that, for both  $2\pi$  and  $4\pi$ -kinks, the bounds on the parameter regions for existence given by the preceding theory are in fact sharp. Section 4 simulates the time-dependent lattice equations, to test for stability of solutions, and finally Sec. 5 draws conclusions.

## 2 Existence of kinks

### 2.1 Embedded soliton theory

Champneys and Kivhsar [8] studied the model (5) via a quasi-continuum approximation. This non-rigorous method is valid in the limit that  $d$  is small. See also [21] for more general quasi-continuum approximations to lattice differential equations. The idea is to replace the second-difference operator in

(3) by a Taylor expansion in space. Keeping the first two terms in the Taylor series would lead to the Klein-Gordon equation (4). At next-order one obtains

$$u_{tt} - u_{xx} - \frac{\gamma}{12}u_{xxxx} + W'(u; \alpha) = 0. \quad (7)$$

Note that this fourth-order operator is unbounded, leading to an artificial short-wavelength instability when studying the *dynamics* of (7). This may be removed by considering an extra 6th-order spatial derivative or a fourth-order mixed spatio-temporal derivative terms. However, since our purpose is to examine the *existence* properties only, the fourth-order form (7) is sufficient. Travelling waves of (7) with phase speed  $s$  are governed by the equation

$$\frac{\gamma}{12}u_{zzzz} + (1 + s^2)u_{zz} - W'(u; \alpha) = 0, \quad (8)$$

where  $z = x - st$ , and kinks are heteroclinic solutions with boundary conditions (6).

In [8] it was argued that, since for all  $\gamma > 0$  the linearisation of (8) about zero yields saddle-centre eigenvalues (a pure imaginary pair and a pure real pair) then the theory of embedded solitons applies [9,33]. That is, solitons are of codimension-one in the  $(s, \gamma, \alpha)$  parameter space. The ‘solitons’ in this case are kinks with topological charge  $Q = |m_2 - m_1|$ , according to the boundary conditions (6). We shall call such solutions  $2Q\pi$ -kinks, and for definiteness take  $m_2 \geq m_1 = 0$ .

It was shown in [8] that there are no  $2\pi$ -kinks for (8) with  $\alpha = 0$ , but a set of discrete curves in the  $(s, \alpha)$ -plane at which  $4\pi$ -kinks occur. These kinks’ profiles have monotonic decay and are symmetric about their midpoint at which  $u = \pi$ , with each kink identified by the number of small oscillations around this midpoint. The simplest  $4\pi$ -kink is monotonic and has the explicit form [2]

$$u(z) = 8 \tan^{-1} \exp \left\{ (\gamma/4)^{1/4} z \right\}, \quad \text{where,} \quad s^2 = 1 - \frac{\sqrt{\gamma}}{3}.$$

This relation between  $s$  and  $\gamma$  is plotted as a dashed line (the outermost one) in Fig. 4 below, as are three other branches of  $4\pi$ -kinks found numerically in [8]. Note that all branches can be continued into the limit  $s \rightarrow 0$ . Also for each  $4\pi$  solution one can appeal to the theory of Mielke, Holmes and O’Reilly [24] that gives the existence of a sequence of parameter values that converge exponentially to that of the kink in question at which  $6\pi$ -kinks exist. More generally there are similar sequences of  $2(n + 1)\pi$ -kinks converging on each  $2n\pi$ -kink for all  $n \geq 2$ . Moreover, in the case of a purely harmonic potential  $W(u; \alpha = 0)$  the same theory gives the existence of kink-antikink pairs which are regular ( $Q = 0$ ) solitons. However, this does not show the existence of  $2\pi$ -kinks ( $Q = 1$ ). In fact, there are none for  $s > 0$ . (The theory of [22]

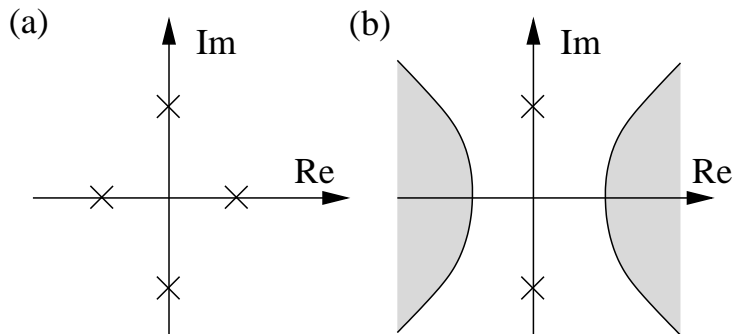


Fig. 1. Necessary condition on the spectrum of the linearised travelling-wave equation for the existence of codimension-one kink solutions for: (a) a fourth-order ODE model; (b) an infinite-dimensional advance-delay equation where the shading represents the region of the complex plain where the rest of the infinite discrete spectrum lies.

suggests that one reason for the existence of  $4\pi$ -kinks is that they are formed as boundstates of two  $2\pi$ -*quasi-kinks* without the need for the existence of any truly localised  $2\pi$ -kinks. By tuning the separation between the two quasi-kinks, their oscillatory tails can be made to exactly cancel.) In this paper therefore we shall focus only on  $2\pi$  and  $4\pi$ -kinks, because the existence of higher-order multi-kinks (and kink/anti-kink pairs) will follow immediately.

## 2.2 A necessary condition for codimension-one kinks

Now, what does the above quasi-continuum theory tell us about the full advance-delay equation (3)? Well, the crucial point about the embedded soliton theory is that in order to find codimension-one kinks one needs the equilibrium at 0 to have only one pair of eigenvalues on the imaginary axis. That is, the stable and unstable manifolds are  $(N - 1)$ -dimensional where  $2N$  is the dimension of the underlying phase space. The advance-delay equation can be thought of a dynamical system with an infinite-dimensional phase space. Unlike PDEs such systems have discrete spectrum only (eigenvalues) so the analogy with ODEs is much stronger, and we can apply the same criterion (see Fig. 1(b)). This criterion is equivalent to saying that the dispersion relation of (3) should support a single branch of linear waves (so-called phonons). To see this note that the dispersion relation is given by substituting  $u = \exp(i\Omega t - \Lambda x)$  into (3):

$$\Omega^2 = 2(1 - \cos \Lambda) + \gamma(1 + 2\alpha).$$

The phase speed of linear waves is  $s = \Omega/\Lambda$  leading to the equation

$$s^2\omega^2 = 2(1 - \cos \omega) + \gamma(1 + 2\alpha), \quad (9)$$

where the spatial wavelength  $\Lambda$  has been replaced by  $\omega$ . This substitution has been made so as to make plain that (9) is in fact the condition for a pair of

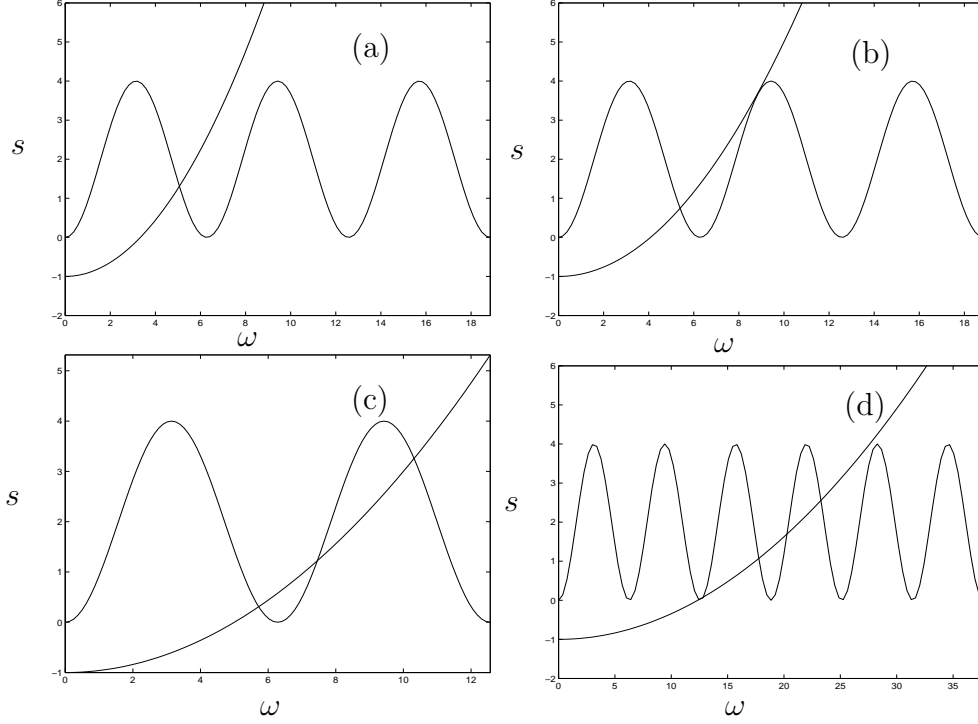


Fig. 2. Graphical construction of solutions to (9) for fixed  $\gamma(1+2\alpha) = 1$  but increasing  $s$ : (a) a unique solution for  $s$  sufficiently large; (b) a double root; (c) multiple solutions when  $s$  is sufficiently small; (d) further double roots as  $s$  is decreased. Note that the number of roots increases in (a-d) from 1 to 5 (counting multiplicity).

imaginary eigenvalues  $\pm i\omega$  of the linearisation of the advance-delay equation (5). The equation (9) has a simple graphical interpretation. It can be rewritten in the form

$$s^2\omega^2 - \gamma(1+2\alpha) = 4\sin^2(\omega/2), \quad (10)$$

where we can consider separately the graphs of the left-hand and right-hand sides as a function of  $\omega$  – see Fig. 2 for the indicative value  $\gamma(1+2\alpha) = 1$ .

Suppose  $\gamma(1+2\alpha) > 0$  is fixed and  $s \neq 0$ . The right-hand side of (10) is non-negative and bounded, while the left-hand side is negative for small  $\omega$  but tends to  $+\infty$  as  $\omega \rightarrow \infty$ . So there is at least one solution for all  $s$ . Clearly for  $s$  sufficiently large this solution will be unique, as the intersection point between the two curves will occur for  $\omega < \pi/2$  (Fig. 2(a)). For smaller  $s$  we may get multiple solutions (Fig. 2(c)). These extra solutions are created (or destroyed) when there is a quadratic tangency between the left and right-hand sides (Fig. 2(b)). For sufficiently small  $s$  there will be further tangencies and many solutions (Fig. 2(d)). It follows that the condition for a double root to (9) is that in addition

$$s^2\omega = \sin\omega \quad (11)$$

is satisfied.

In Fig. 3(a) we have plotted loci of solutions in the  $(\gamma, s)$ -plane to equations

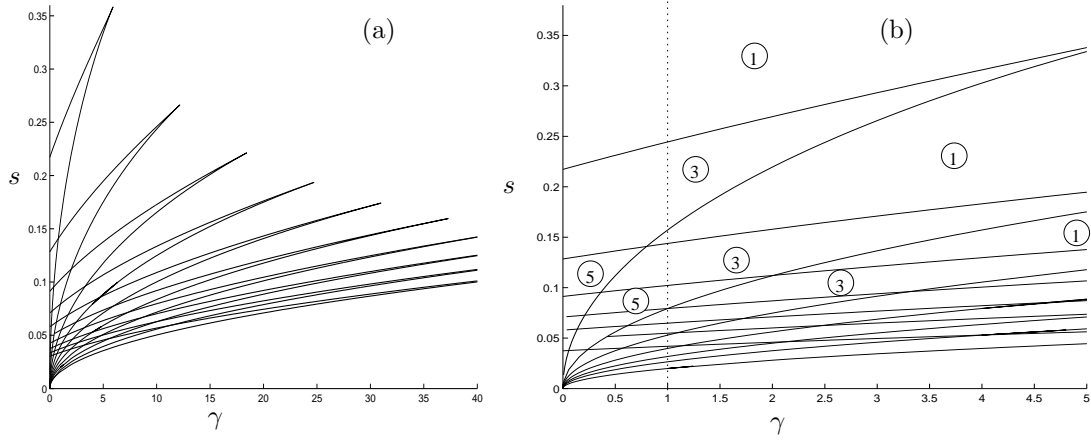


Fig. 3. (a) Plot of the loci of double roots of (9) for varying  $\gamma$  and  $s$ . (b) A close-up for small  $s$ , with the number of positive roots inside various parameter regions indicated. *The ‘new barrier’ to the existence of moving kinks given in the title of this paper stems from the fact that the number of positive roots increases to infinity as  $s \rightarrow 0$*

(10) and (11) defining multiple roots, and also indicated the corresponding number of pairs of imaginary eigenvalues in open parameter regions. This figure is for the case  $\alpha = 0$ , but the diagram also applies for non-zero  $\alpha$  after the transformation  $\gamma \mapsto \gamma/(1 + 2\alpha)$ .

Consider Fig. 3 for fixed  $\gamma$ . According to the above theory, codimension-one embedded kinks may only exist when there is a single pair of imaginary eigenvalues (a single positive root of (9)). For sufficiently large  $s$  this condition is true. As  $s$  is reduced, we cross successive ‘multi-phonon bands’ where additional pairs of imaginary eigenvalues occur. Inside each multi-phonon band we may at best expect to see quasi kinks, with non-decaying oscillatory tails which in fact will exist throughout the whole parameter plane. As we shall see in Sec. 3.1 below, truly localised kinks are just a special case of such solutions, that happen to have zero tail oscillation. However, we should not expect any truly localised kinks inside the multi-phonon bands except at discrete values in a three-parameter system.

Eventually, for sufficiently small  $s$  these bands overlap until we see a lower bound  $s = s_l(\gamma)$  such that for all  $s < s_l$  there always exist more than one pair of imaginary eigenvalues, and hence codimension-one embedded kinks cannot occur. This lower bound then forms a *new barrier* that prevents the existence of codimension-one kinks for small wavespeeds.

Moreover it is clear from Fig. 3(a) that the bands accumulate on  $s = 0$  in such a way that for each  $\gamma > 0$ , the number of overlapping bands increases as  $s \rightarrow 0$ . Hence the existence of a true embedded kink all the way down to  $s = 0$  would be of infinite codimension. In other words, for all values of  $\alpha, \gamma > 0$  *there is always a lower bound on the wave speed of true embedded kinks.*

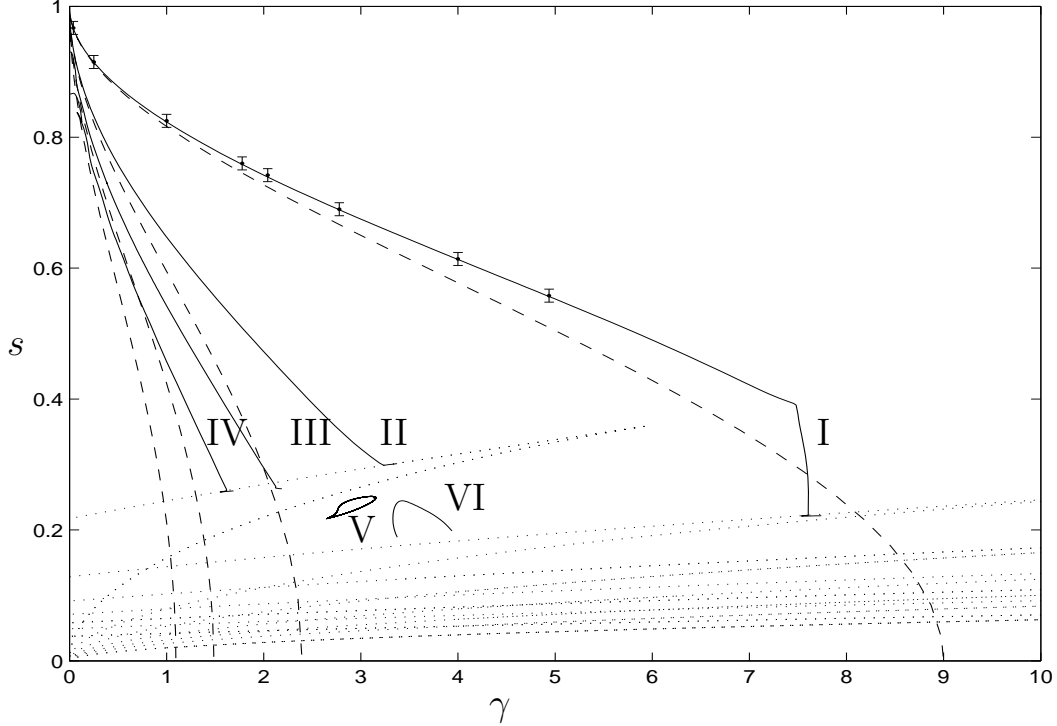


Fig. 4. Wave speed versus  $\gamma$  for four different kink solutions with vanishing tail ( $\Delta = 0$ ). The eight dots with error bars at branch I represent numerical data from Peyrard and Kruskal [26]. Solid lines represent our numerical results and the dashed lines the corresponding results by Champneys and Kivshar [8]. The multi-phonon bands are shown as dotted lines, compare with Figure 3.

Figure 4, which computes numerically branches of  $4\pi$ -kinks for  $\alpha = 0$  and which shall be explained in more detail in the next Section, shows that this lower bound in fact appears to be sharp. That is, branches of truly localised kinks terminate at the boundary of the first encountered multi-phonon bands upon decreasing  $s$ . Other branches may also exist inside the gaps between multi-phonon bands. Note also that  $s = 1$  appears to be a strict upper bound for all truly travelling kinks. This shall not concern us any further, the main aim of this paper being the establishment of a lower bound on  $s$ .

Incidentally, it is worthwhile to point out that the linearisation of the advance-delay equation (5) possesses a single pair of purely *real* eigenvalues  $\pm\lambda$ , provided  $\gamma(1 + 2\alpha) > 0$ . Here  $\lambda$  is given by the unique positive solution to

$$s^2\lambda^2 + \gamma(1 + 2\alpha) = 4\sinh^2(\lambda/2). \quad (12)$$

All the other (infinitely many) eigenvalues of the advance-delay operator are complex. Now, it is reasonable to conjecture by analogy with the fourth-order operator case (see Fig. 1 that this real eigenvalue governs the exponential decay to zero of the tails of true kinks. However, as is well known, the dominant behaviour in the tail should generically be given by the non-imaginary eigen-

value that is closest to the imaginary axis. Clearly, close to a multi-phonon boundary the dominant eigenvalue must be complex (since a pair are about to coalesce on the imaginary axis). If embedded kinks exist right up to the boundary of a multi-phonon band then their tail behaviour should become non-monotonic.

### 2.3 The singular limit $s \rightarrow 0$ .

The limit  $s = 0$  is highly singular. This is the stationary kink problem, and the advance-delay equation (5) becomes a discrete two-dimensional map. Numerically it is easy to show that there are just two (up to phase shift)  $2\pi$ -kinks. These have either site-centred symmetry (with a lattice point at  $u = \pi$ ) or bond-centred symmetry (lattice points placed symmetrically about  $u = \pi$ ). In the mapping, this represents the transverse intersection of the stable and unstable manifolds of the saddle point at  $u = 2n\pi$ . Then we can apply the Smale Birkhoff homoclinic theorem to show the existence of infinitely many  $2n\pi$ -kinks for all  $n \neq 1$ . Fig. 5 provides a numerical illustration of the case  $\gamma = 1$ , which is typical of the situation for each fixed  $\gamma \neq 0$ . Here the unstable manifold of the origin is computed. Every piece of this manifold that intersects the line  $u_n - u_{n-1} = 0$  represents, by symmetry, a bond-centred kink solution. Site-centred kinks may similarly be constructed by finding intersections with the line  $u_n = 0 \pmod{2\pi}$ .

Consider the singular perturbation for  $s > 0$ . A plausible physical argument states that moving  $2\pi$ -kinks with infinitesimal wave speed can only exist if the difference in energy between the bond-centred and lattice-centred stationary modes, the so-called Peierls-Nabarro barrier, vanishes. Savin *et al.* [29] computed this energy barrier as a function of  $\alpha$  and  $\gamma$  (which is the reciprocal of their parameter  $\kappa$ ). They found that when  $\alpha = 0$ , the barrier remains positive. However, for fixed  $\alpha$  sufficiently large one finds a sequence of values of  $\gamma$  at which the barrier vanishes. We reproduce in Table 1 their results for  $\alpha = 1$ . Note that approximately the barrier vanishes in an approximately linear sequence of values of  $\sqrt{1/\gamma_i}$ . Similar linear sequences are obtained (with different constant spacings) if you examine the data in [29, Table 1] for  $\alpha = 0.1$  and  $\alpha = \infty$ . However the sequence terminates much more quickly for smaller  $\alpha$  (no points  $\gamma_i$  for  $\alpha = 0$ , fourteen points for  $\alpha = 1$  and a seemingly infinite sequence for  $\alpha = \infty$ .)

These numerical results would suggest the codimension-one persistence of moving  $2\pi$ -kinks, bifurcating from the limit  $s = 0$  at precisely these  $\gamma$ -values. At first sight this would appear akin to the codimension-one persistence of embedded solitons of partial differential equations in [7], which relies on the normal-form theory of [23]. However, the details of such a theory have yet to be

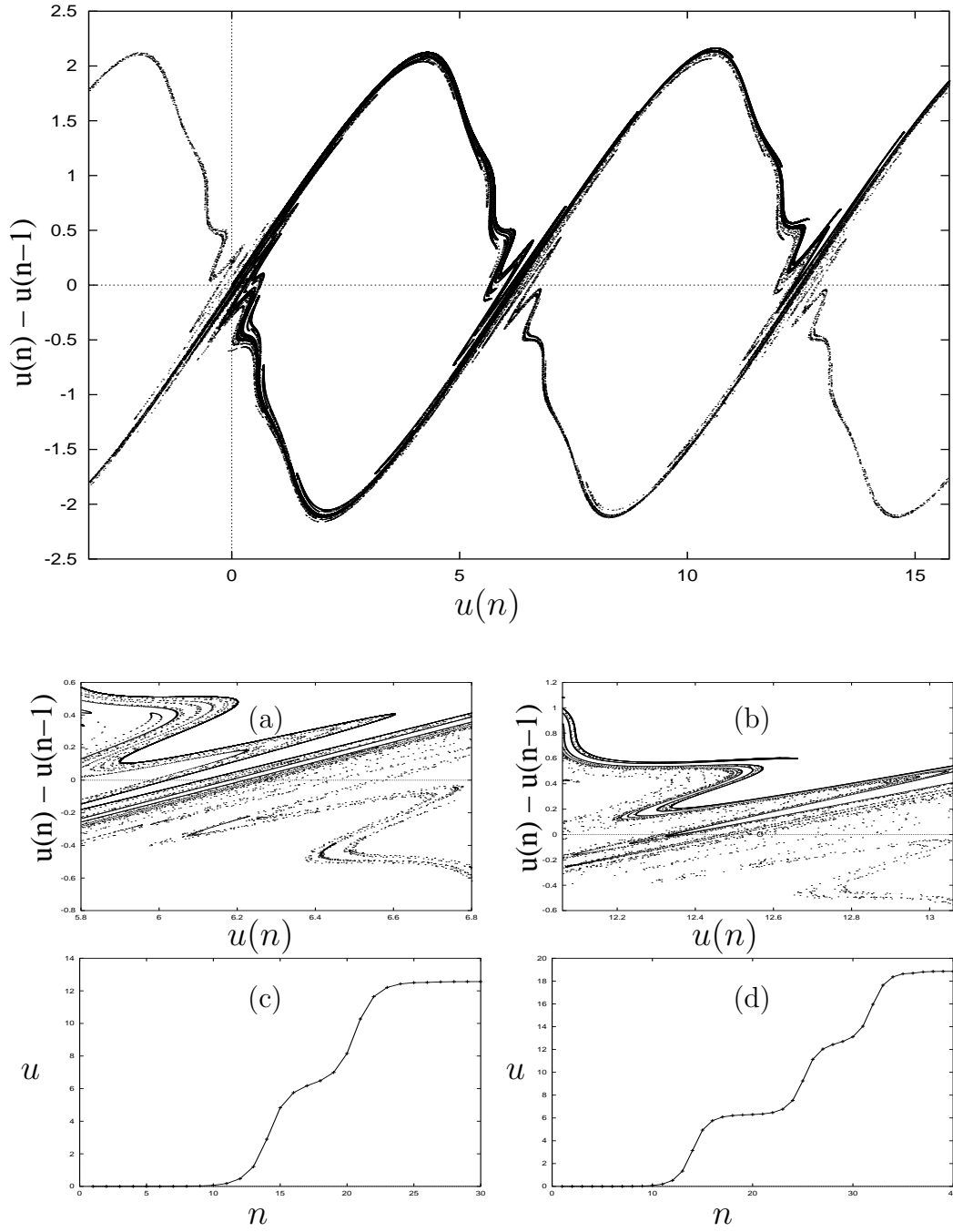


Fig. 5. Construction of stationary multi-kink solutions by computation of the unstable manifold of the fixed point  $u = 0$  of the two-dimensional map (5) with  $s = 0$ . Panels (a) and (b) show close-ups near  $u = 2\pi$  and  $4\pi$  where intersections with  $u = 2n\pi$  or  $u_n - u_{n-1} = 0$  correspond to the existence of multi-kinks. Panels (c) and (d) show representative examples of the families of  $4\pi$  and  $8\pi$ -kinks so constructed.



$n$	$1/\gamma_n$	$\sqrt{1/\gamma_n}$	$\sqrt{1/\gamma_n} - \sqrt{1/\gamma_{n-1}}$
1	0.2667	0.5164	-
2	0.7872	0.8572	0.341
3	1.6140	1.2704	0.730
4	2.7470	2.0450	0.774
5	4.1819	3.0396	0.388
6	5.9186	2.0629	0.388
7	7.9575	5.6740	0.389
8	10.2993	3.2092	0.388
9	12.9440	3.5977	0.389
10	15.8918	3.9864	0.389
11	19.1430	4.3752	0.389

Table 1

Values of  $1/\gamma$  for which the Peierls-Nabarro barrier vanishes for  $\alpha = 1$  (from [29]), together with a scaling of these results. The first column gives the index of the vanishing of the barrier in order of decreasing  $\gamma$ .

worked out for lattice equations. Also the system here has odd symmetry and the unperturbed is a  $2\pi$ -kink, rather than an algebraically small homoclinic orbit. However, the central result of that theory is a linear sequence of values of a parameter, akin to  $\sqrt{1/\gamma}$  in this case, in which true embedded solitons (kinks) appear out of the singular limit. We mention the work of Iooss and co-workers [19], and of Feckan and Rothos [15] for the first rigorous theory in this direction for lattice equations. Other methods to prove existence for related equations were established in [17].

We must point though to another limitation of applying the above theory to the limit  $s \rightarrow 0$  (we note that the singular limit in [15] is  $\gamma \rightarrow 0$  for  $s$  sufficiently large). The theory is suggestive that, for  $\alpha$  sufficiently large,  $2\pi$ -kinks bifurcate at discrete  $\gamma$ -values from  $s = 0$ . But this precisely contradicts the results of the previous subsection, which shows the existence of an infinite-codimension barrier. We now turn to numerics to resolve this potential discrepancy.

### 3 Numerical results: existence

#### 3.1 Numerical method

Methods for solving advance-delay boundary-value problem like 5 are few and far between. Shooting will not work since the initial value problem makes no sense. One idea is to use a modification to finite difference boundary-value solvers which enables the data at  $z + 1$  and  $z - 1$  to be accessible to the linear solver [1]. Another approach, which is especially suited to second-order problems like (5) is to use a pseudospectral method [14]. We shall adopt this latter approach, specifically an adaptation to the method used in [29].

As in [29], we approximate the kink solutions by functions  $u(z)$  on a long finite interval  $[-L/2, L/2]$  that are odd about their mid point using a Fourier sine expansion. However, for kinks that connect  $2m_1\pi$  to  $2m_2\pi$ , we have uneven boundary conditions

$$u(-L/2) = 2m_1\pi \quad \text{and} \quad u(+L/2) = 2m_2\pi,$$

and, as is a common technique in pseudospectral methods (see Boyd [4]), we chose an appropriate odd function  $u_0(z)$  that satisfies the boundary condition and apply the spectral method to the residual. That is we set

$$u(z) \approx u_0(z) + \sum_{j=1}^N c_j \phi_j(z), \quad (13)$$

where

$$\phi_j(z) = \sin\left(\frac{2\pi j z}{L}\right) \quad (14)$$

and  $c_j \in \mathbb{R}$  are the coefficients of the sine expansion. Following [35], we use a profile  $u_0(z)$  which is a close approximation to a  $2Q\pi$ -kink solution for  $Q = 1$  or  $2$ :

$$u_0(z) = Q\pi + \frac{Q\pi}{2} \left( \tanh\left[\nu\left(z - \frac{\delta}{2}\right)\right] \tanh\left[\nu\left(z + \frac{\delta}{2}\right)\right] \right). \quad (15)$$

Here  $\nu$  and  $\delta$  are parameters that are determined once only before the computation of the residual, with  $\delta = 0$  being chosen *a priori* in the case of a monotonic kink. Here,  $\nu$  is a measure of the slope of the initial guess and  $\delta$  is a measure of the spacing between the outer and inner region of the kink for a non-monotonic solution.

Substitution of (13), (14) into (5) yields

$$F(z) = \sum_{j=1}^N \left[ \phi_j(z+1) - 2\phi_j(z) + \phi_j(z-1) + s^2 \left( \frac{2\pi j}{L} \right)^2 \phi_j(z) \right] c_j - V'(z, \phi_j, c_j) = 0, \quad (16)$$

which corresponds to a nonlinear system of  $N$  algebraic equations for the  $N$  unknown coefficients  $c_j$ , given the  $N$  collocation points  $z_i = \frac{Li}{2(N+1)}$ .

To find a solution to (16) at fixed parameter values, the globally convergent Powell hybrid method is used [28] with an error tolerance of  $10^{-16}$ . A starting solution for the coefficients was the trivial guess  $\mathbf{c} = (1, 0, \dots, 0)$ . This solution is then used as a starting solution in the software AUTO [12], which can be used to continue solutions to an algebraic system of equations, described by  $F(\mathbf{c}; \sigma) = 0$ . Here  $\mathbf{c}$  is the  $N$ -dimensional vector of coefficients  $c_j$  and  $\sigma$  is whichever of  $\gamma$ ,  $\alpha$  or  $s$  is chosen to be the continuation parameter.

Since, in general, solutions are quasi-kinks we need to introduce an auxiliary equation that enables us to find the exact  $\sigma$ -value for which the tail vanishes. We do this by seeking simple zeros of

$$\Delta = u\left(\frac{L}{2}\right) - u\left(\frac{LN}{2(N+1)}\right), \quad (17)$$

where  $f = u(z)$  describes the kink solution. This function effectively represents a signed measure of the derivative of the solution at its right-hand end point. Hence, since the boundary conditions demands the solution value be zero there, this is a signed measure of the amplitude of the periodic tail, which becomes exact in the limit  $L \rightarrow \infty$  (see [10] for an application of a similar method to find embedded soliton solutions of an infinite-dimensional water-wave problem.) In the implementation in [29,35], minimisation of the  $L_2$ -norm of the tail region was used as a measure of the tail oscillations. The condition (17) has the advantage over this in that vanishing tails are found as a regular zero of  $\Delta$ , and so may be used as part of the continuation problem. In particular we can solve

$$F(\mathbf{c}; \sigma_1, \sigma_2) \quad (18)$$

in tandem with (17), where now  $\sigma_{1,2}$  are any two of the parameters  $\gamma$ ,  $\alpha$ ,  $s$  and  $\Delta$ . If a zero of  $\Delta$  is detected along a branch of quasi-kinks, then  $\Delta = 0$  can be frozen and branches of true kinks followed in two parameters, typically either  $(\gamma, s)$  or  $(\alpha, s)$ .

In what follows all results were obtained using  $L = 40$  and  $N = 100$ .

### 3.2 Quasi-kinks (kinks with oscillatory background)

Figure 6 shows the result of continuation of four different branches of  $4\pi$ -quasi-kinks for fixed wave speed  $s = 0.6$  and  $\alpha = 0$ , with  $\gamma$  and  $\Delta$  allowed to vary. Solutions at isolated points along branches I–IV were found by taking the initial  $\delta$  in (15) to be a little greater than 1.0–4.0 respectively.

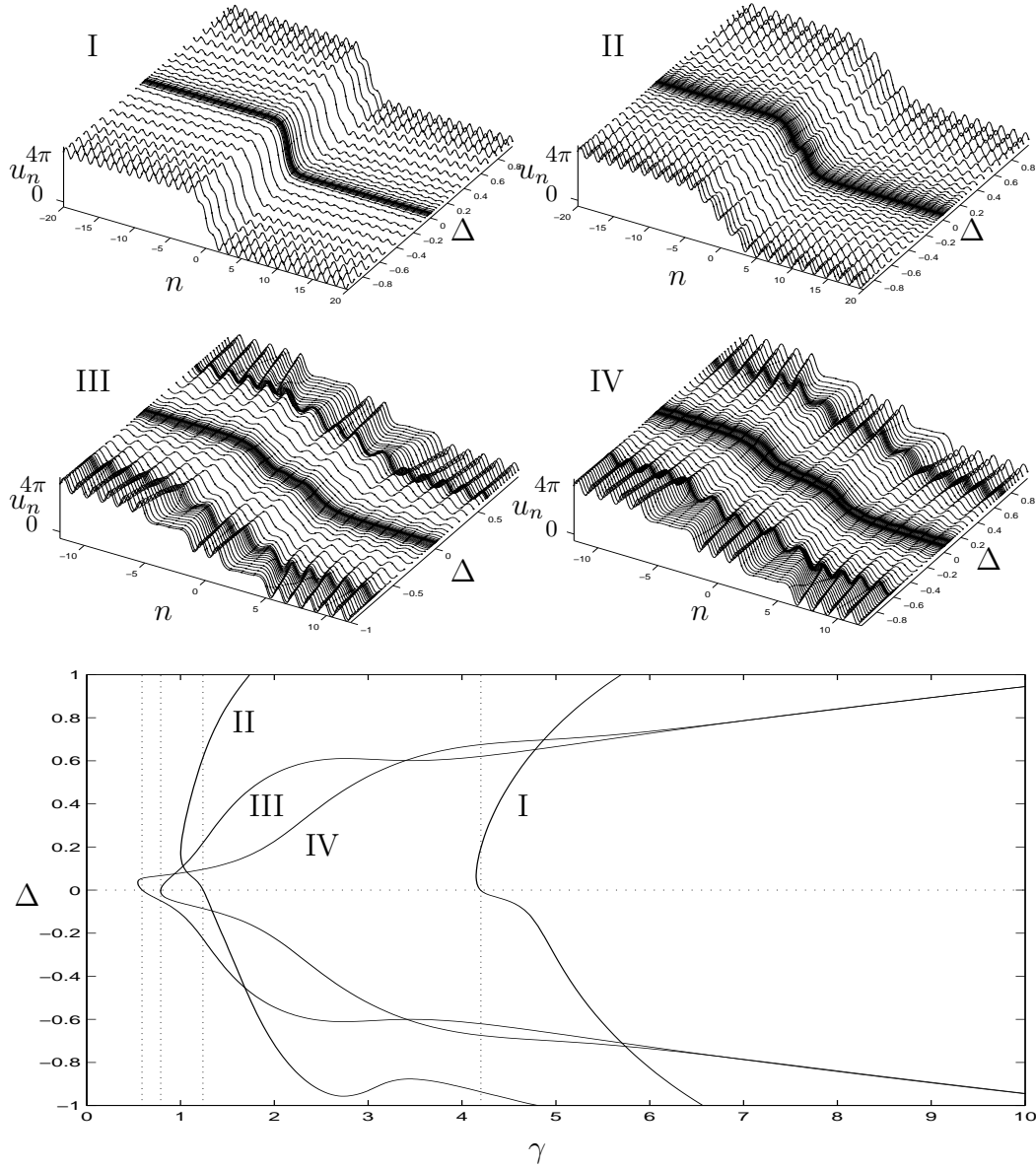


Fig. 6. The lower plot shows the tail end condition  $\Delta$  versus  $\gamma$  for the four different kink solutions labelled I–IV in Fig. 4, for fixed  $s = 0.6$  and  $\alpha = 0$ . Dotted lines pick-out  $\gamma$ -values for which there are zeros of  $\Delta$ . The upper panels show a sequence of snap-shot solution profiles as the parameters vary along each of the continuation branches. Note that here and in subsequent similar plots, profiles are only plotted every few steps of the continuation process. The spacing of solutions in the diagram therefore indicates the step lengths selected by the continuation algorithm.

Note that each of these four branches possesses a zero of  $\Delta$ . These correspond to the existence of an embedded kink solution within this continuum of quasi-kinks. Note the change in phase in the tail of the quasi-kink, consequent on the change of sign of  $\Delta$ . It should also be noted that we are not computing the full family of quasi-kinks. At each value of  $\gamma$  there will in fact be a complete one-parameter family of quasi-kinks which can be parametrised by the

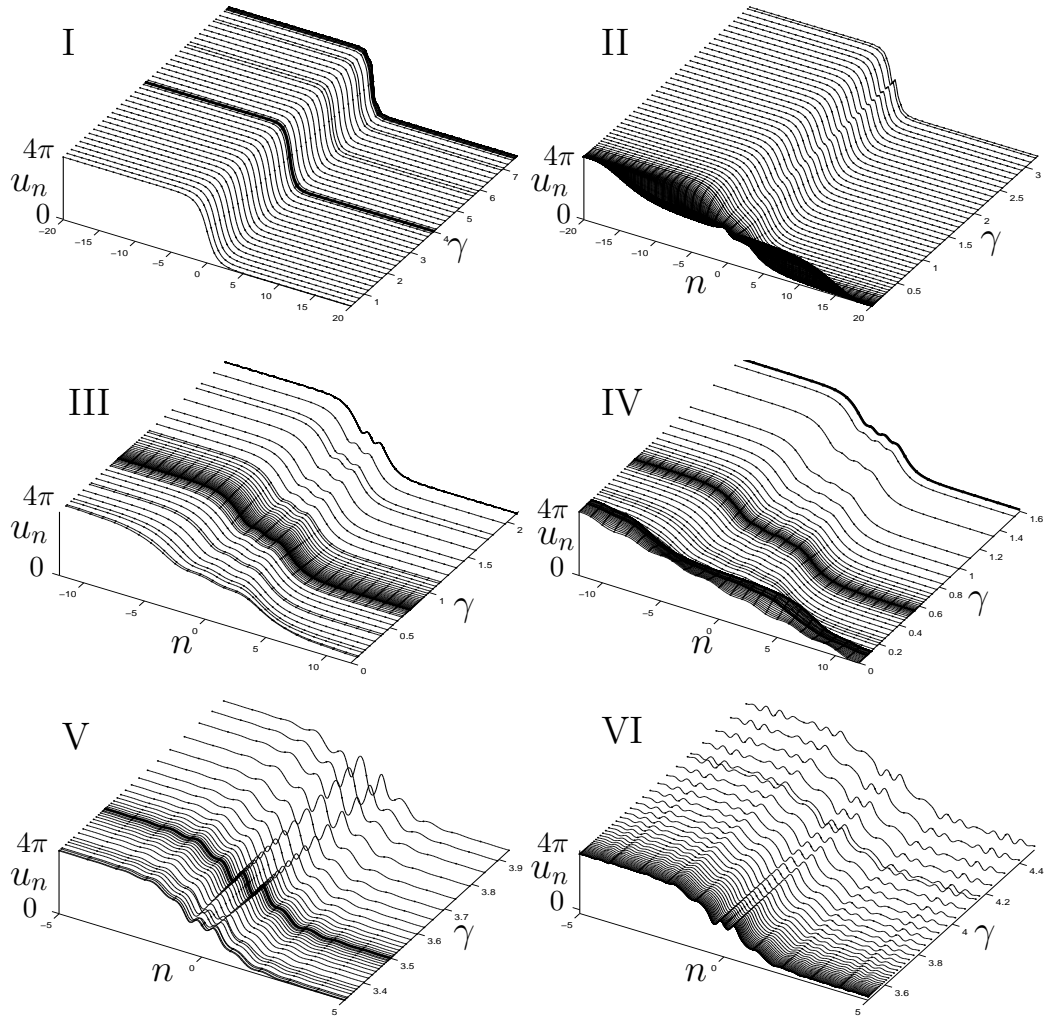


Fig. 7. Solution profiles along the six continuation branches of  $4\pi$ -kinks plotted in Fig. 4 with  $\alpha = \Delta = 0$  and  $\gamma$  and  $s$  varying.

phase-shift between the two oscillatory tails. By fixing the length of the computational interval,  $L$  we are in effect fixing this phase shift. However, when the amplitude of the tails vanish, then the phase shift is meaningless, so that all sufficiently long intervals  $L$  will pick up such solutions. Precisely this methodology was used in [10] for finding true solitary water waves embedded within branches of quasi-solitons.

### 3.3 $4\pi$ -kinks

Recall Figure 4. The first four branches represent continuation in  $\gamma$  of the kink solutions at the four zeros of  $\Delta$  in Fig. 6. Note the branch I is precisely that computed (at discrete  $\gamma$ -values) by Peyrard and Kruskal. Also there is good agreement with the quasi-continuum theory of [8] which should only be

valid as the continuum limit  $\gamma \rightarrow 0$  is approached. In particular, in agreement with that theory we find precisely four branches (labelled I–IV) that can be followed into the limit  $s \rightarrow 0$ . These results are more or less identical to those obtained previously in [29]. The solution profiles on the four branches are shown in Fig. 7, where we can see that the solutions differ qualitatively in the width (and number of oscillations) in the shelf between the two bound-state  $2\pi$ -kinks. The initial point on each branch of branches I–IV was obtained with the Powell hybrid method, by letting  $\delta$  in equation (15) be greater than 1–4 respectively.

Note that, up to numerical precision, each of these four branches terminates at the boundary of a multi-phonon band. In particular for this  $\alpha$ -value, the branch I narrowly misses the ‘nose’ of the first multi-phonon band before terminating on the upper boundary of second multi-phonon band. Nevertheless the branch appears to feel the effect of the first multi-phonon band, leading to the strange corner in the branch that was also observed in [29] but not explained there.

In addition to these four branches we have also found evidence of kinks existing inside the gaps between the multi-phonon branches (labelled VI and V in Fig. 4). These solutions lie on isolated branches, or *isola*. Profiles of the corresponding solutions in Fig. 7, suggest that at least branch VI may not be a true embedded kink, but that a longer interval  $L$  is required to resolve the behaviour of the tail.

Figure 8 shows continuation results for fixed  $\gamma$  and varying  $\alpha$  for branches I and II as well as continuation results in  $\gamma$  for  $\alpha = 4$ . These results are summarised in a three dimensional plot in the parameter space  $(s, \gamma, \alpha)$  shown in Fig. 9, which shows the influence of the multi-phonon bands on the solutions. In particular, which band the branch terminates on in the  $(\gamma, s)$ -plane clearly varies with  $\alpha$ . When the termination point is close to the nose of one of the bands, then complex looping structures may be born in the branch, like for branch I when  $\alpha = 4$ . Presumably the pinching-off of such loops under further variation of  $\alpha$  may be an explanation for the isolas we found with the gaps between multi-phonon bands.

### 3.4 $2\pi$ -kinks

Figure 11 shows the continuation results for the  $2\pi$  kinks found in [29] for fixed  $\gamma = 1$ . It is clear from this Figure that kink I terminates at the contact with the first phonon band, but kink II resides inside one of the multi-phonon bands (the 10th). The explanation may be that branch II is really a quasi-kink but that it has a very small component in its tail of the eigenvector corresponding

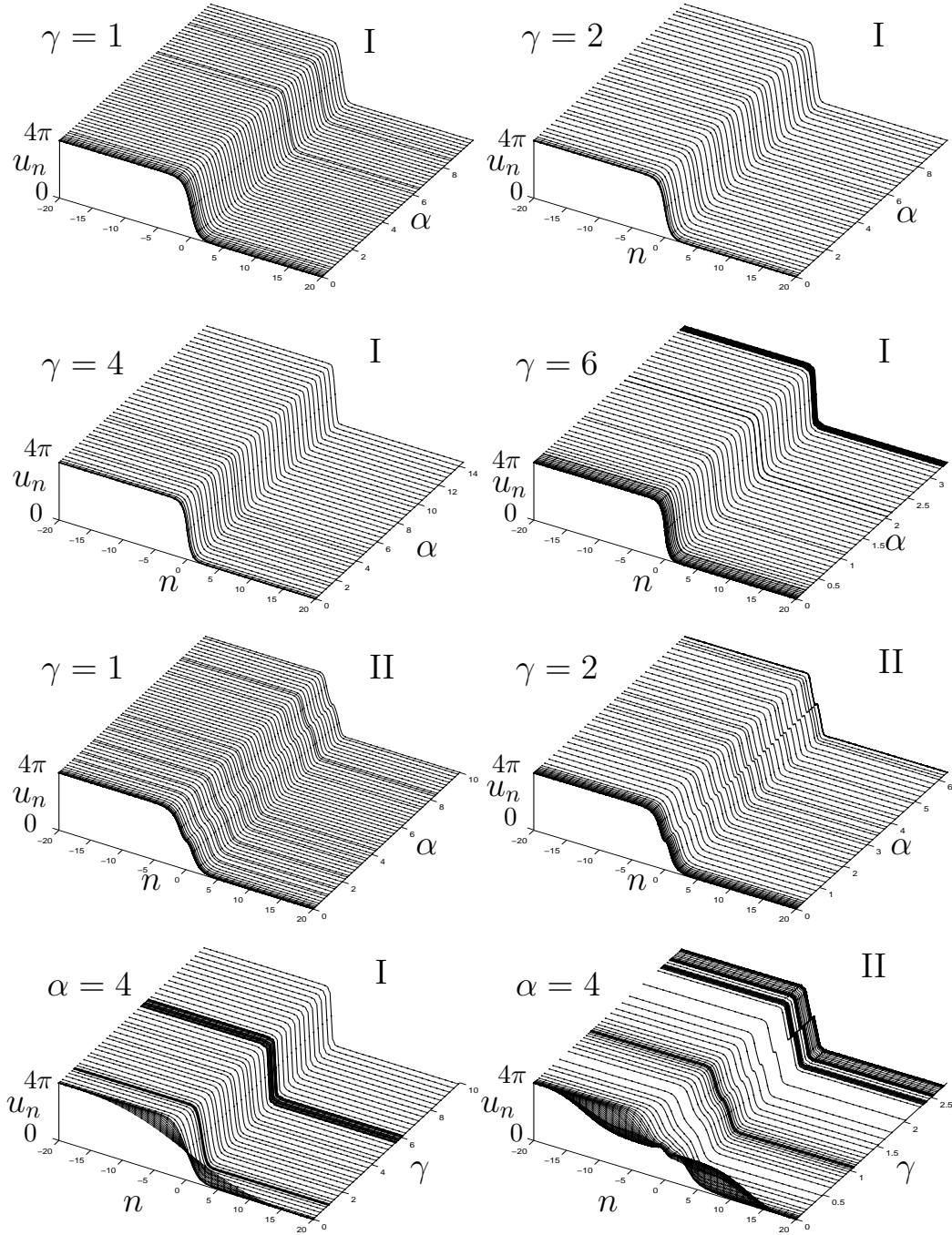


Fig. 8. Plot of the solutions along the continuation in  $\alpha$  for the  $4\pi$ -kinks I and II of Fig. 4 for constant  $\gamma$  and two continuations of kinks I and II in  $\gamma$  for  $\alpha = 4$ .

to the 10th multi-phonon band. The plots in Fig. 12 show the solution profiles along each of these two branches. There is no visible oscillation in the tail of branch II, but they are potentially too small to detect for this small  $s$ -value. Fig. 12 also shows results of continuation of these solutions in  $\alpha$ . The continuation results are summarised in a three dimensional plot in parameter space  $(s, \gamma, \alpha)$  shown in Fig.13.

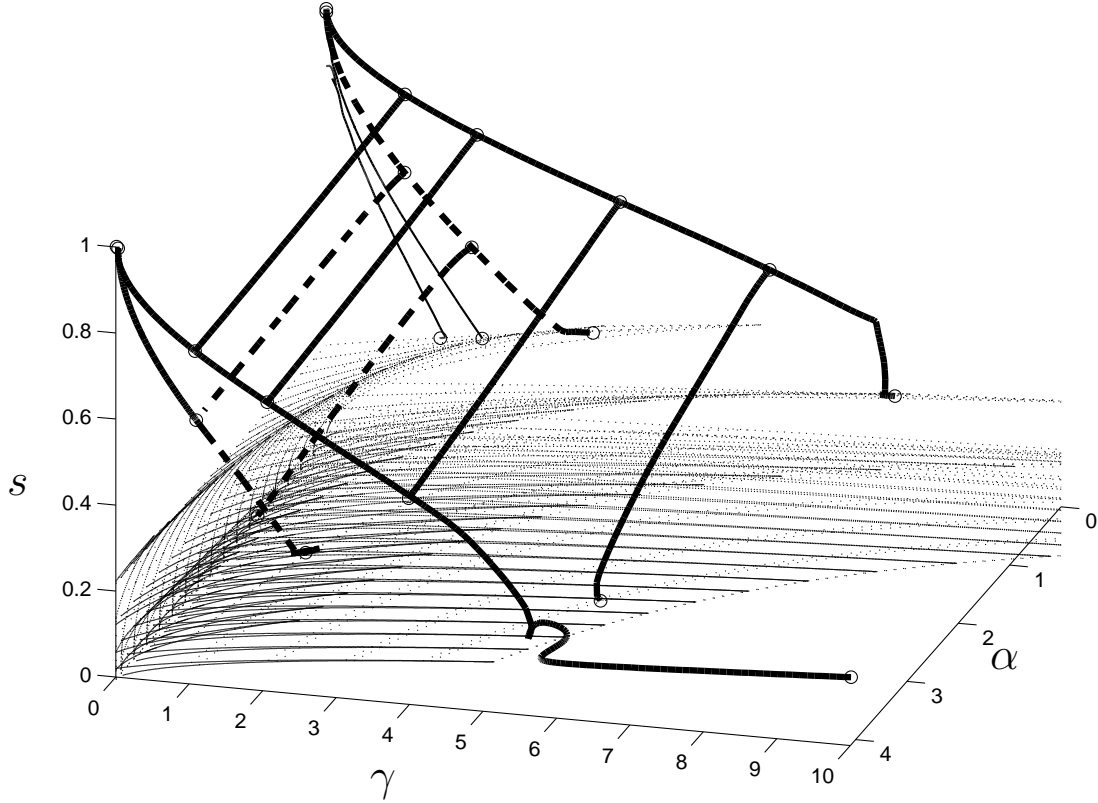


Fig. 9. A three-dimensional plot of the continuation results in the parameter space  $(s, \gamma, \alpha)$  for the first two  $4\pi$ -kinks only (I solid line, II dashed line). The multi-phonon bands are denoted by dotted lines and describe surfaces in parameter space. Note that for simplicity only some of the multi-phonon bands are plotted.

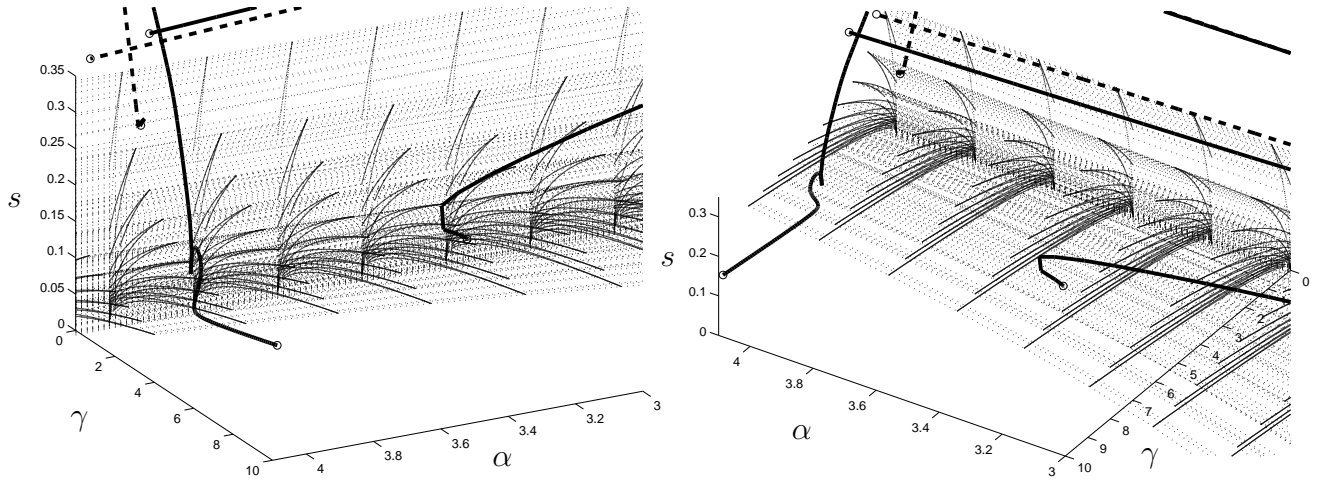


Fig. 10. Blow-up of Fig. 9 from different angles.

For fixed  $s$  and  $\alpha = 1$  one can look for kink solutions with vanishing tails in varying  $\gamma$  and finds for  $s = 0.5$  four  $2\pi$  kinks which are shown in Fig. 14. In the same figure we have plotted on the  $s = 0$ -axis the  $\gamma$  values that correspond to the ‘transparent points’ of Table 1. Note that these computed solutions each



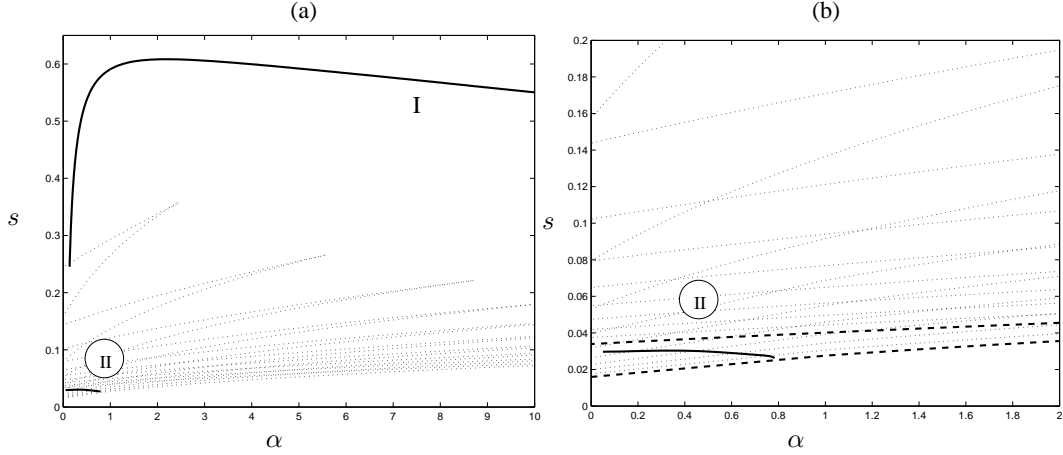


Fig. 11. (a) Continuation results for the  $2\pi$ -kinks with  $\gamma = 1$  fixed and (b) a blowup of the region around kink II. Dashed lines show the boundaries of the multi-phonon bands, with the bold dashed lines in (b) representing the 10th multi-phonon band.

terminate approximately at the edge of a multi-phonon band. With reduced tolerance in the continuation algorithm it is possible to continue through some of the bands. These curves are shown as dashed lines in Fig. 14. However, the dashed curves were found not to be repeatable under continuation in the reverse parameter direction, nor under increased tolerance. We conclude that there are branches of quasi-kinks within the multi-phonon band that have small but non-zero oscillations within their tails.

Note that the results are consistent with the suggestion that once a branch crosses a multi-phonon band, then within the band there continues a branch of quasi-kinks which have no component in the direction of *the leading* imaginary eigenvalues in their tail. The oscillations associated with the higher multi-phonon bands may be extremely small. These branches of ‘almost’ kinks presumably persist all the way down to  $s = 0$  crossing more and more phonon branches as they do so, generating more and more components of oscillatory modes, albeit with almost vanishingly small amplitude. They then reach  $s = 0$  at the indicated transparent points.

#### 4 Numerical results: stability and dynamics

To integrate in time the system of equations for each of  $M$  lattice points, we use a Runge-Kutta method with local and global error control and apply it to the first-order system of ODEs

$$\dot{u}_n(t) = v_n(t), \quad \text{and} \quad \dot{v}_n(t) = u_{n+1} - 2u_n + u_{n-1} - \gamma W'(u_n), \quad n = 1 \dots M \quad (19)$$

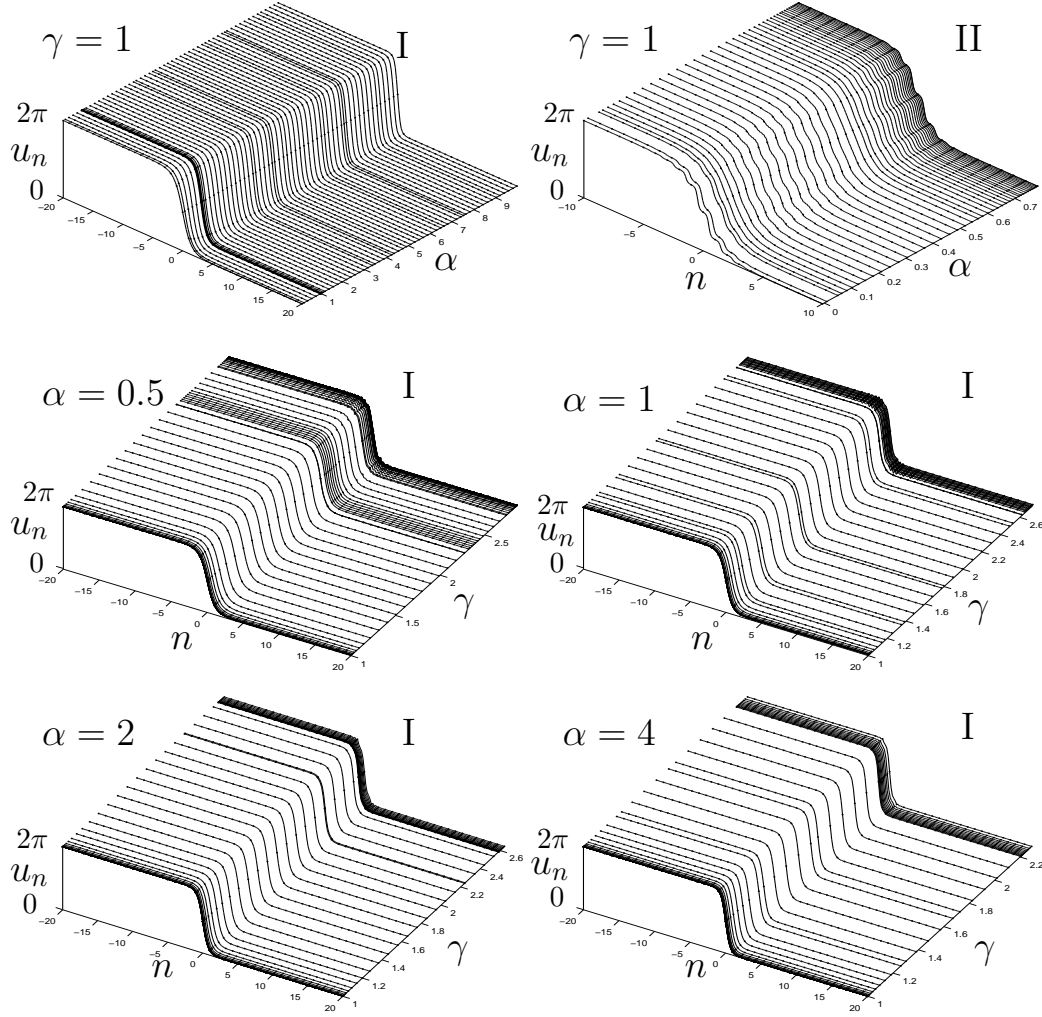


Fig. 12. Solution profiles of  $2\pi$ -kinks along the continuation branches in  $\alpha$  and in  $\gamma$  for the fixed values of the other parameter indicated (see Figs. 11 and 13).

with periodic boundary conditions. An initial time step of  $\Delta t = 1 \cdot 10^{-3}$  was enough to ensure convergence and in practice about  $10^6$  steps were taken to integrate, which amounted to roughly  $2.5 \times 10^6$  evaluations as the cost of the integration.  $M$  was chosen to be 200 and the kink solutions obtained from the continuation were interpolated to the lattice points and the remaining lattice points padded with appropriate values to obtain a starting solution to  $u_n(t = 0)$  to (19).  $\dot{u}_n(t = 0)$  was obtained by differentiating the pseudospectral approximation given by

$$\dot{u}_n(t) = \frac{dz(n, t)}{dt} \frac{du(z)}{dz} = -s \left\{ u'_0(z) + \sum_{j=1}^N c_j \phi'_j(z) \right\}, \quad (20)$$

where  $dz(n, t)/dt = -s$ . A time integration over 400–800 seconds was sufficient to study the temporal behaviour of the solutions.

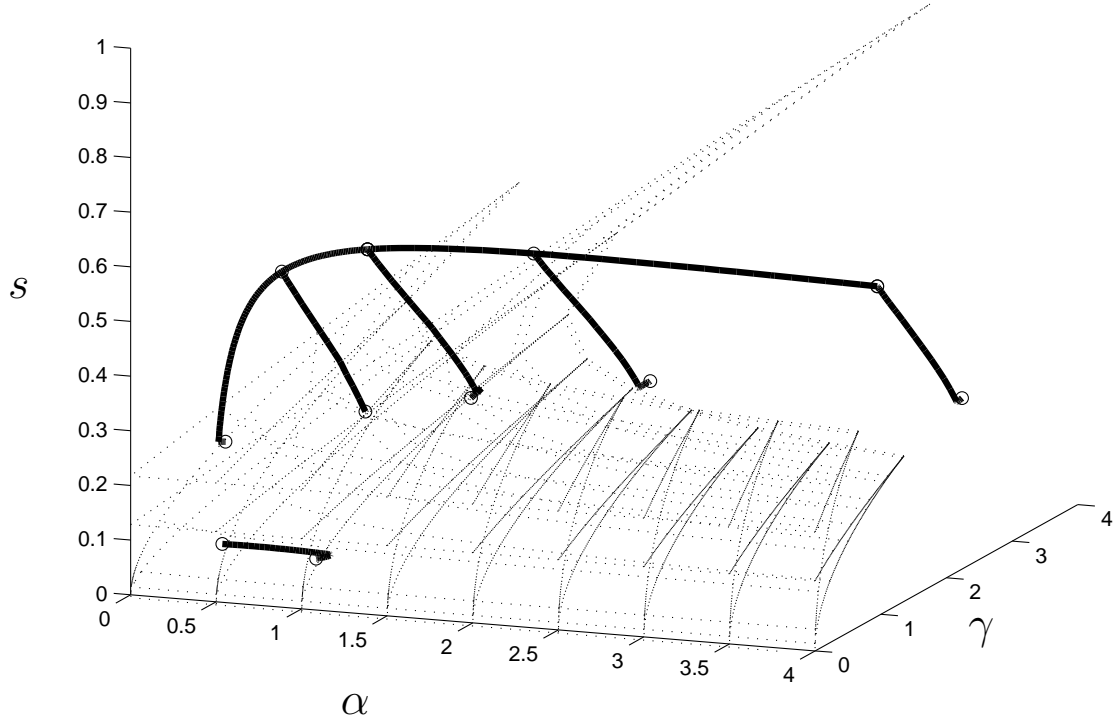


Fig. 13. A three-dimensional plot of the continuation results in the parameter space  $(s, \gamma, \alpha)$  for the  $2\pi$ -kinks. The multi-phonon bands are denoted by dotted lines and describe surfaces in parameter space. Note that for simplicity only some of the multi-phonon bands are plotted.

Figure 16 shows the results for the temporal integration of the system of ODEs given by (19) for the  $4\pi$ -kink solutions I,II,III,IV and V for the parameter values shown in the Figure. No artificial perturbation was added other than that introduced by the discretisation and numerical method. It is clear from these results that the  $4\pi$ -kinks are largely stable; that is, coherent structures close to the original kink evolve up to the end times. This echoes the conclusions of [29]. However, there is here the suggestion that some of the higher-order  $4\pi$ -kinks (with more oscillations in the shelf between the two  $2\pi$ -kinks) may in fact be weakly unstable since small amounts of radiation appear to be being generated in the tails. Figure 17 shows the simulation results for the two  $2\pi$  kinks I and II which would appear to be quite stable. The question of whether these solutions are truly stable is left for future investigation, we refer to the work of [20,18] for rigorous mathematical results on related questions.

Figure 18 shows the time evolution of the stable  $4\pi$ -kink I, with periodic boundary conditions, where the initial wave speed is set to  $\dot{u}_n = 0$ . Our previous results show that no stable  $4\pi$ -kink exists in the neighbourhood of  $s = 0$  because of the resonances with the multi-phonon bands. We observe from

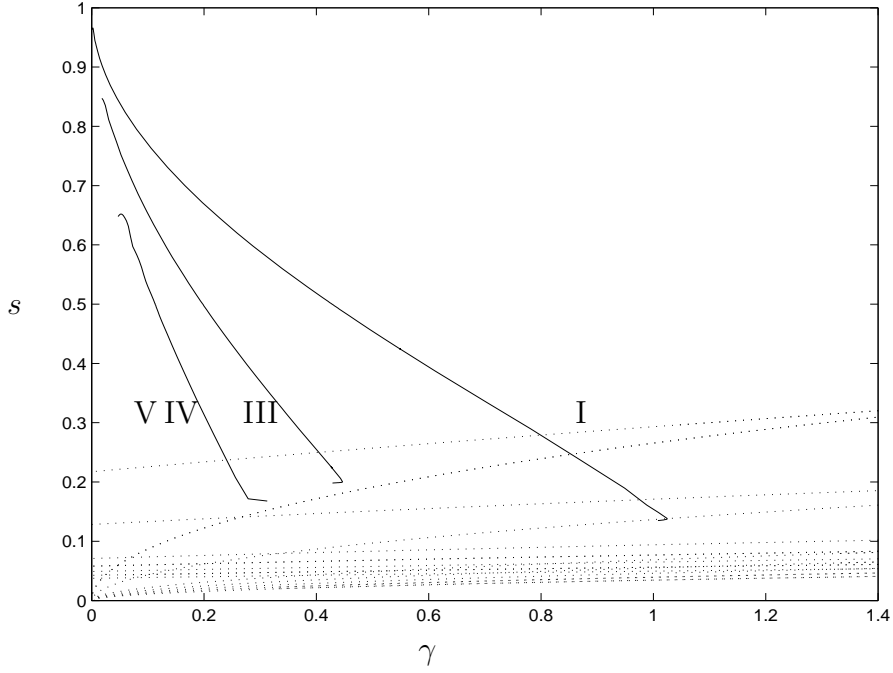


Fig. 14. Continuation results for the  $2\pi$ -kinks, for  $\alpha = 1$  and varying  $\gamma$ .

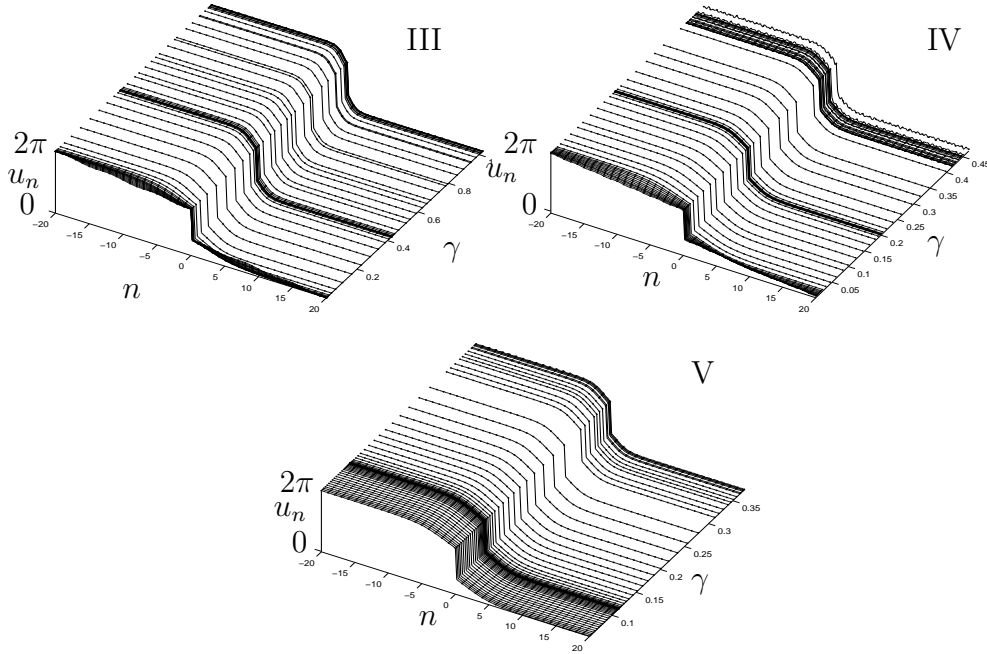


Fig. 15. Solution profiles along the continuation branches shown in Fig. 14 for kinks III, IV, V.

the Figure that this is reflected in the  $4\pi$ -kink breaking up into two separate  $2\pi$ -kinks with opposite velocities. They are subsequently attracted to each other, possibly by interaction through their tails, and go through subsequent near inelastic collision. Similar behaviour is also observed in [29] for the collision of two  $2\pi$ -kinks traveling in opposite directions. However in that case,

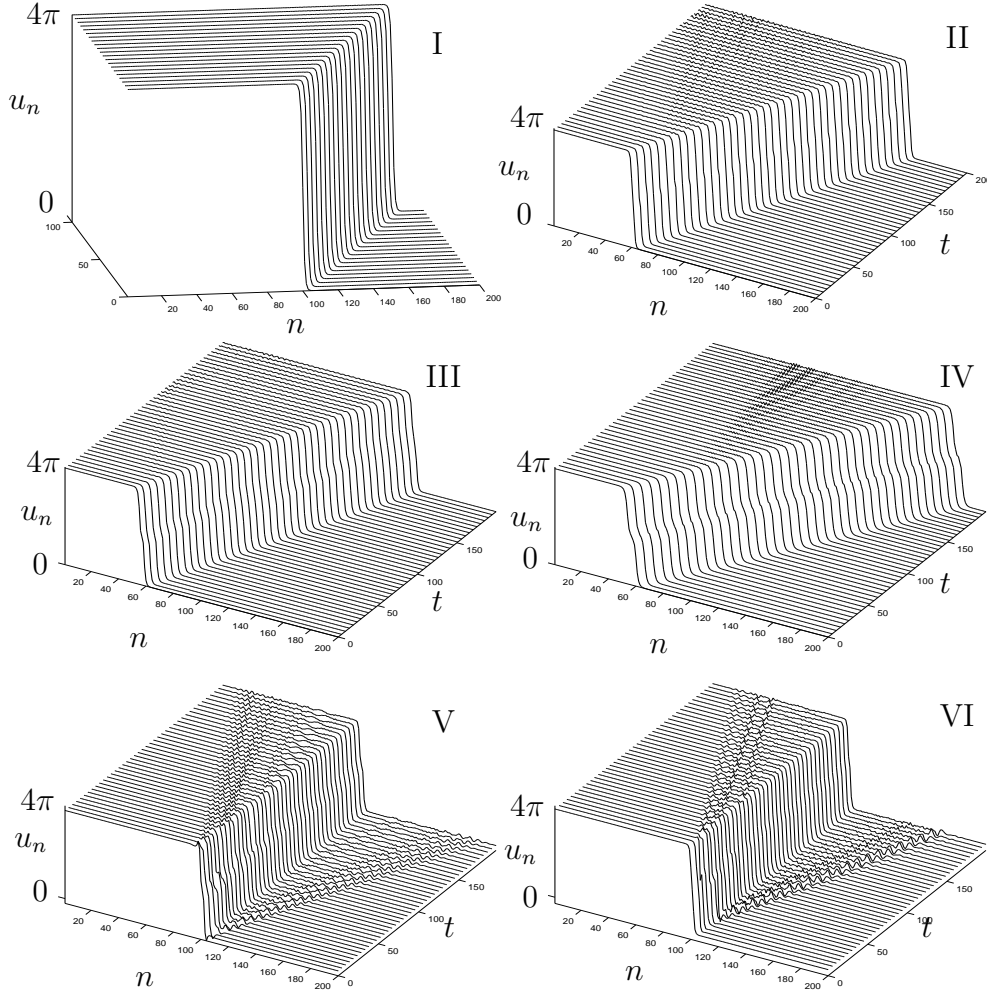


Fig. 16. Results for the time evolution of moving  $4\pi$ -kinks of the full lattice equation (3) with  $\alpha = 0$ . Solution labels I–V correspond to those in Fig. 4. The plots are specifically for: I  $(s, \gamma) = (0.823, 1)$ ; II  $(0.4724, 2)$ ; III  $(0.4157, 1.5)$ ; IV  $(0.6166, 0.55)$ ; V  $(0.25, 3.156)$  and VI  $(0.242, 3.5)$ .

the two kinks recombine to form a bound state  $4\pi$ -kink. For movie visualizations of various stable and unstable travelling  $4\pi$ -kinks (IV and V) visit <http://www.enm.bris.ac.uk/anm/preprints/2003r01.html>.

## 5 Conclusion

In this work we have highlighted the existence of a lower bound on the wavespeed of moving kinks in FK lattices. This lower bound (the ‘new barrier’ of the title) comes about because as one approaches wavespeed  $s = 0^+$  we find the accumulation of infinitely many resonances with linear waves. Each resonance means that an additional free parameter would need to be taken in order to find the presence of truly localised kinks (i.e. they become of higher

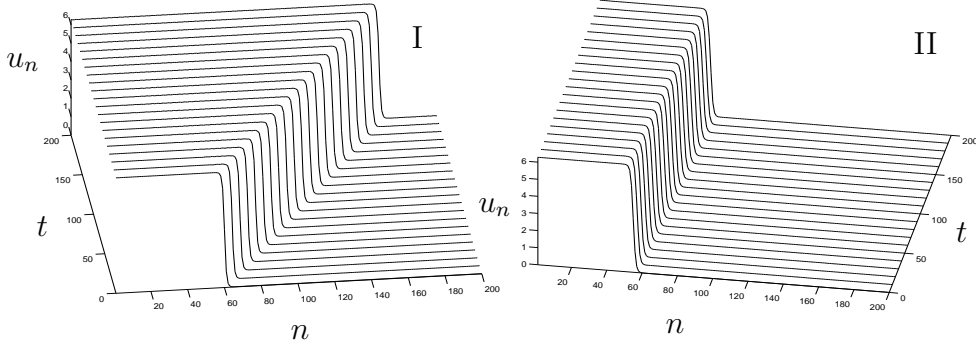


Fig. 17. ODE results for the  $2\pi$ -kinks I:  $s = 0.537$ ,  $\alpha = 0.5$ , II:  $s = 0.0324$ ,  $\alpha = 0.5$  and  $\gamma = 1$  in both cases.

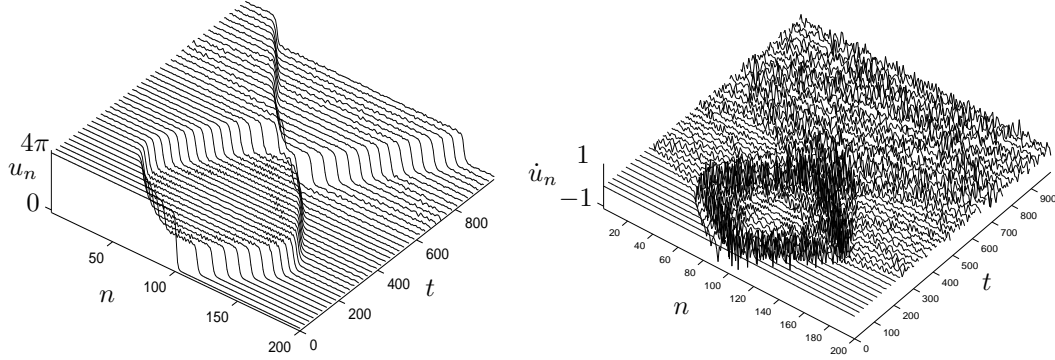


Fig. 18. Results for the time evolution of the stable  $4\pi$ -kink I with  $\alpha = 0$ ,  $\gamma = 1$  and periodic boundary conditions, but with the velocity set to  $\dot{u}_n = 0$ . Compare with Figure 16.

and higher codimension). Our numerical results reveal this bound to be sharp in that branches of localised kinks are found to terminate at the boundaries of the multi-resonance regions of parameter space (so called multi-phonon bands).

This, the main conclusion of the paper, explains why in previous work (such as Fig. 12 of [26]) that, although numerical data has been extrapolated to suggest kinks can travel with arbitrary small velocity, no such kinks have ever been computed. In contrast, kinks on an oscillatory background, so called quasi-kinks, (which have questionable physical validity) can occur in a large open region of parameter space, with arbitrary wavespeeds.

Our computational strategy was strongly inspired by the pioneering work of Eilbeck and collaborators [14,13,29,35], who introduced the idea of using pseudospectral methods to solve the advance-delay equation satisfied by travelling kinks of permanent form. We have adapted their method to put it in a continuation framework with a truly localised kink occurring as the zero of a regular boundary condition, while computing a branch of quasi-kinks. We would like to emphasise the generality of the pseudospectral approach, which can deal

with a much more general class of advance-delay equations by a change of basis function. For example we would like to note that for a first derivative in time it would be easy enough to enlarge the set of basis functions to include even functions and thus be able to proceed along the same numerical method outlined here. In fact any type of advance-delay equation can be dealt with by appropriate choice of basis function, see Boyd [4] and literature cited therein.

Also, crucially we have explained the termination of continuation curves of moving  $4\pi$  and  $2\pi$  kinks of generalised sine-Gordon lattices, which were previously observed to end ‘in mid air’ (see Figs. 6 and 14 of [29]). Moreover, in Fig. 4 we have shown how our results agree with earlier computations, both the numerical simulation results of Peyrard and Kruskal and the quasi-continuum approximation of [8].

Although we have focused on a particular family of nonlinear potentials  $W(u; \alpha)$ , the analytical arguments and numerical methods we have introduced are applicable to a wide class of nonlinear FK lattice models. Future work will look at the case where the inter-site potential encompasses longer-range interactions, and can be nonlinear [25]. It should be noted that the methodology based on the dispersion relation for finding the lower-bound on the kink velocity is a purely linear criterion and will not be affected by these added complications and thus holds universally. Also, since we have posed the problem within a framework of numerical continuation with regular boundary conditions, many more of these problems may be addressed by continuation in homotopy parameters that interpolate between the simple sine-Gordon lattice and the problem at hand. A final, crucial open question is to seek rigorous mathematical proof of our non-existence results.

### *Acknowledgements*

The authors would like to thank Michel Peyrard for giving us access to his numerical data for reproduction in Fig. 4, and also Yaroslav Zolotaryuk for sharing details of his numerical implementation. We also acknowledge useful conversations with Jonathan Wattis, Sebius Doedel, Yuri Kivshar and Boris Malomed. The work was supported by EPSRC grant GR/R02719/01, and that of ARC was partially supported by an EPSRC Advanced Fellowship.

### **References**

- [1] K. A. Abell, C. E. Elmer, A. R. Humphries, and E. S. Van Vleck. Computation of mixed type functional differential boundary value problems, 2003. <http://www.maths.sussex.ac.uk/Staff/ARH/Research/TW>.

- [2] M. M. Bogdan and A. M. Kosevich. Radiationless motion of one-dimensional solitons in dispersive media. In K. Spatschek and F.G. Mertens, editors, *Nonlinear Coherent Structures in Physics and Biology*, pages 373–376, New York, 1994. Plenum.
- [3] J.P. Boyd. *Weakly nonlocal solitary waves and beyond-all-orders asymptotics*. Kluwer, Dodrecht, 1998.
- [4] J.P. Boyd. *Chebyshev and Fourier spectral methods*. Dover, 2nd edition, 2001.
- [5] O. M. Braun and Y. S. Kivshar. Nonlinear dynamics of the Frenkel-Kontorova model. *Phys. Rep.*, 306:1–108, 1998.
- [6] O.M. Braun, A.R. Bishop, and Röder. Hysteresis in the underdamped driven Frenkel-Kontorova model. *Phys. Rev. Lett.*, 79:3692–3695, 1997.
- [7] A. R. Champneys. Codimension-one persistence beyond all orders of homoclinic orbits to singular saddle centres in reversible systems. *Nonlinearity*, 14:87–112, 2000.
- [8] A. R. Champneys and Yu. S. Kivshar. Origin of multikinks in dispersive nonlinear systems. *Physical Review E*, 2551-2554:61, 2000.
- [9] A. R. Champneys, B. A. Malomed, J. Yang, and D. Kaup. Embedded solitons: solitary waves in resonance with the linear spectrum. *Physica D*, 152-153:340–354, 2001.
- [10] A. R. Champneys, J.-M. Vanden-Broeck, and G. J. Lord. Do true elevation solitary waves exist? A numerical investigation. *J. Fluid Mech.*, 454:403–417, 2002.
- [11] J. F. Currie, J. A. Krumhansl, A. R. Bishop, and S. E. Trullinger. Statistical mechanics of one dimensional solitary wave-bearing scalar fields: Exact results and ideal gas phenomenology. *Phys. Rev. B*, 22:477–496, 1980.
- [12] E. J. Doedel, A. R. Champneys, T. R. Fairgrieve, Yu. A. Kuznetsov, B. Sandstede, and X. J. Wang. AUTO97 continuation and bifurcation software for ordinary differential equations, 1997. Available by anonymous ftp from FTP.CS.CONCORDIA.CA, directory /DOEDEL/AUTO.
- [13] D. B. Duncan, J. C. Eilbeck, H. Federsen, and J. A. D. Wattis. Solitons on lattices. *Physica D*, 68:1–11, 1993.
- [14] J. Eilbeck and R. Flesch. Calculation of families of solitary waves on discrete lattices. *Phys. Lett. A*, 149:200–202, 1990.
- [15] M. Feckan and V. Rothos. Bifurcations of periodics from homoclinics in singular ode: Applications to discretizations of travelling waves of pde. *Comms. Pure Appl. Analysis*, 1:475–483, 2002.
- [16] J. Frenkel and T. Kontorova. On the theory of plastic deformation and twinning. *Acad. Sci. U.S.S.R. J. Phys.*, 1:137–149, 1939.



- [17] G. Friesecke and J. A. D. Wattis. Existence theorem for solitary waves on lattices. *Commun. Math. Phys.*, 161:391–418, 1994.
- [18] G. G. Friesecke and R. L. Pego. Solitary waves on FPU lattices: II. Linear implies nonlinear stability. *Nonlinearity*, 15:1343–1359, 2002.
- [19] G. Iooss and K. Kirchgässner. Traveling waves in a chain of coupled nonlinear oscillators. *Comm. Math. Phys.*, 211:439–464, 2000.
- [20] P. G. Kevrekedis and M. I. Weinstein. Dynamics of lattice kinks. *Physica D*, 142:113–152, 2000.
- [21] P. G. Kevrekidis, I. G. Kevrekidis, A. R. Bishop, and E. S. Titi. Continuum approach to discreteness. *Physical Review E*, 65:art. no. 046613, 2002.
- [22] K. Kolossovski, A. R. Champneys, A. V. Buryak, and R. A. Sammut. Multi-pulse embedded solitons as bound states of quasi-solitons. *Physica D*, 171:153–177, 2002.
- [23] E. Lombdari. *Oscillatory integrals and phenomena beyond all algebraic orders*. Springer-Verlag, Berlin, 2000. Lecture Notes in Mathematics 1741.
- [24] A. Mielke, P. Holmes, and O. O’Reilly. Cascades of homoclinic orbits to, and chaos near a Hamiltonian saddle centre. *J. Dynamics Differential Eqns*, 4:95–126, 1992.
- [25] S. F. Mingaleev, Y. B. Gaididei, E. Majernikova, and S. Shpyrko. Kinks in the discrete sine-Gordon model with Kac-Baker long range interactions. *Phys. Rev. E*, 61:4454–4461, 2000.
- [26] M. Peyrard and M. D. Kruskal. Kink dynamics in the highly discrete sine-Gordon system. *Physica D*, 14:88–102, 1984.
- [27] M. Peyrard and M. Remoissenet. Soliton-like excitations in a one-dimensional atomic chain with a nonlinear deformable substrate potential. *Phys. Rev. B*, 26:2886–2899, 1982.
- [28] M. J. D. Powell. “A hybrid method for nonlinear algebraic equations”, in numerical methods for nonlinear algebraic equations, 1970. Gordon and Breach.
- [29] A. V. Savin, Y. Zolotaryuk, and J. C. Eilbeck. Moving kinks and nanopterons in the nonlinear Klein-Gordon lattice. *Physica D*, 138:267–281, 2000.
- [30] J.M. Speight and R.S. Ward. A discrete  $\phi^4$  system without a Peierls-Nabarro barrier. *Nonlinearity*, pages 475–484, 1997.
- [31] A. V. Ustinov. Solitons in Josephson junctions. *Physica D*, 123:315–329, 1998.
- [32] A. V. Ustinov, B. A. Malomed, and S. Sakai. Bunched fluxon states in one-dimensional josephson junction arrays. *Phys. Rev. B*, 57:11691–11697, 1998.
- [33] J. Yang, B. A. Malomed, D. J. Kaup, and A. R. Champneys. Embedded solitons: a new type of solitary wave. *Mathematics & Computer Simulation*, 56:585–600, 2001.

- [34] V.E. Zakharov and E.A. Kuznetsov. Optical solitons and quasisolitons. *J. Exp. Theo. Phys*, 86:1035–1046, 1998.
- [35] Y. Zolotaryuk, J. C. Eilbeck, and A. V. Savin. Bound states of lattice solitons and their bifurcations. *Physica D*, 108:81–91, 1997.